DR ISABELLE I SALLES-CRAWLEY (Orcid ID : 0000-0001-7394-0587)

Article type : Original Article

Title:

Defective fibrin deposition and thrombus stability in *Bambi^{/-}* mice is mediated by elevated anticoagulant function

Short Title: Endothelial BAMBI's role in thrombus stability

Authors affiliations:

James T.B. Crawley *, Argita Zalli *, James H. Monkman *, Anastasis Petri, David A. Lane *, Josefin Ahnström *, & Isabelle I. Salles-Crawley *

*Centre for Haematology, Hammersmith Hospital Campus, Imperial College London, London, UK

Correspondence: Dr Isabelle I Salles-Crawley, Centre for Haematology, Imperial College London, Hammersmith Hospital Campus, Du Cane Road, London W12 0NN, UK Tel: +44 (0)20 8383 2298 email: i.salles@imperial.ac.uk

Key words: anticoagulants, endothelial cells, fibrin, mice, thrombomodulin, thrombosis

Type of article: Original Research

This article has been accepted for publication and undergone full peer review but has not been through the copyediting, typesetting, pagination and proofreading process, which may lead to differences between this version and the Version of Record. Please cite this article as doi: 10.1111/jth.14593 This article is protected by copyright. All rights reserved

Essentials

• Bone Morphogenetic and activin membrane-bound inhibitor (BAMBI) is a transmembrane protein highly expressed in platelets and endothelial cells

• Endothelial BAMBI deficiency reduces fibrin accumulation and increases thrombus instability after vascular injury

• The thromboprotective effect is manifest by elevated tissue factor pathway inhibitor (TFPI) and thrombomodulin functions on the endothelium

• TFPI plays an important role in fibrin accumulation in the laser-induced thrombosis model

Summary

Background - BAMBI is a transmembrane protein related to the type I TGF- β receptor family that is present on both platelets and endothelial cells (EC). *Bambi*-deficient mice exhibit reduced hemostatic function and thrombus stability characterized by an increased embolization.

Objective – We aimed to delineate how BAMBI influences endothelial function and thrombus stability.

Methods– *Bambi*-deficient mice were subjected to the laser-induced thrombosis model where platelet and fibrin accumulation was evaluated. Expression of thrombomodulin and TFPI was also assessed in these mice.

Results – Thrombus instability in *Bambi^{/-}* mice was associated with a profound defect in fibrin deposition. Injection of hirudin into *Bambi^{+/+}* mice prior to thrombus formation recapitulated the *Bambi^{-/-}* thrombus instability phenotype. In contrast, hirudin had no additional effect upon thrombus formation in *Bambi^{-/-}* mice. Deletion of *Bambi* in EC resulted in mice with defective thrombus stability caused by decreased fibrin accumulation. Increased levels of the anticoagulant proteins TFPI and thrombomodulin, were detected in *Bambi^{-/-}* mouse lung homogenates. EC isolated from *Bambi^{-/-}* mouse lungs exhibited enhanced ability to activate protein C due to elevated thrombomodulin levels. Blocking thrombomodulin and TFPI *in vivo* fully restored fibrin accumulation and thrombus stability in *Bambi^{-/-}* mice.

Conclusions – We demonstrate that endothelial BAMBI influences fibrin generation and thrombus stability by modulating thrombomodulin and TFPI anticoagulant function of the endothelium, and also highlight the importance of these anticoagulant proteins in the laser-induced thrombosis model.

Introduction

Hemostatic plug formation after vessel injury serves to limit blood loss and maintain vascular integrity. It involves concerted roles of the vessel wall, platelets and other blood cells (e.g. neutrophils, red blood cells), as well as the coagulation cascade.[1-6] Using experimental mouse models of thrombosis, or human blood in *ex vivo* flow assays, previous studies have shown that thrombi exhibit a heterogeneous composition with a core of closely-packed, activated platelets that is overlaid by a shell of less-activated platelets.[3, 7] The core of the thrombus (compared to the shell) has reduced porosity and solute transport that effectively increases the local thrombin concentration leading to more efficient fibrin deposition and thrombus stabilization.[8, 9] Many proteins expressed in the endothelium, platelets and in plasma influence both the formation and stabilization of a thrombus.[10]

Endothelial cells (EC) play a critical role in regulating hemostatic plug formation through production of a variety of thromboprotective agents. These include vasodilators, such as nitric oxide and prostacyclin that also influence platelet function, as well as anticoagulant proteins such as tissue factor (TF) pathway inhibitor (TFPI) and thrombomodulin. TFPI is a Kunitz-type serine protease inhibitor that, together with its cofactor protein S, targets the initiation phase of coagulation by direct inhibition of TF-FVIIa and FXa.[11-13] TFPI exists in two alternatively-spliced isoforms - TFPI α and TFPI β , which are both expressed in EC. In humans, full length TFPIα is primarily secreted into the plasma where it circulates at low concentrations (0.1-0.2nM). Conversely, the shorter TFPI β remains GPI-linked to the endothelial cell surface.[14] Both isoforms inhibit TF-FVIIa in a FXa-dependent manner, with TFPIa likely being more important for regulating hemostasis on platelet surfaces, whereas TFPIß probably functions primarily on the endothelial cell surface to which it is attached.[15] In mice, a shorter soluble TFPI isoform (TFPI γ) consisting of the first two Kunitz domains also exists in circulation.[16-18] Thrombomodulin is a type-I transmembrane protein expressed by EC.[19] Thrombomodulin binds thrombin with

high affinity and enhances the conversion of protein C into activated protein C (APC) by ~1000-fold.[20] In larger vessels, endothelial cell protein C receptor (EPCR) colocalises with thrombomodulin in lipid-rafts and further enhances APC generation (~20 times) by the thrombin-thrombomodulin complex.[21, 22] Once activated, APC proteolytically inactivates FVa and FVIIIa, thereby regulating the propagation phase of coagulation. Modulation of APC activity has recently been shown to influence thrombus formation in a hemophilia mouse model.[23]

BAMBI (bone morphogenetic protein (BMP) and activin membrane-bound inhibitor) is a 260 amino acid transmembrane protein that has been assigned to the transforming growth factor- β (TGF β) superfamily due to the high homology of its extracellular domain to the TGF^β type I receptors (TGF^βRI).[24] It has been postulated that BAMBI antagonizes TGFβ/BMP/activin signaling by preventing the formation of TGF β type I/II receptor heterocomplexes, although the molecular basis of its function remains unclear.[24-26] Interestingly, BAMBI lacks the intracellular kinase domain normally present in TGF^βRI. Furthermore, its intracellular domain shares no homology to any other protein or domain making it difficult to predict the function or mode of action of this domain. BAMBI is highly conserved in vertebrates [24, 27-29] and its transcript is highly expressed in EC and megakaryocytes when compared to other blood cell lineages.[30, 31] Bambi-deficient mice are viable and fertile [32-34] but we have previously reported a proportion of Bambi/- pups dving around weaning age.[34] Bambi^{/-} mice exhibit enhanced angiogenesis in vivo, and are more susceptible to diabetic glomerular disease where an important role of BAMBI in the endothelium was noted. [35, 36] We recently demonstrated that BAMBI acts as a positive regulator of thrombus formation and stability and plays a role in hemostasis.[34] BAMBI deficiency had no effect on platelet count, ex vivo platelet activation, aggregation or procoagulant function, and no influence on the endogenous thrombin potential of plasma. Thrombus formation in Bambi chimeric mice revealed that BAMBI in the vessel wall (rather than in the hematopoietic compartment) was important for thrombus stability.[34] In the present study, we define the mechanisms by which BAMBI in the endothelium (rather that in blood cells, platelets or in extravascular locations) exerts its function and how these influence thrombus formation and stability.

Methods

Generation of Bambi^{flox/flox} Tie2-Cre⁺ mice

All animal work was performed in compliance with Imperial College animal ethics guidelines according to the UK Home Office's Animals (scientific procedures) Act 1986. The *Bambl*^{flox/flox} and *Bambi*^{/-} mice backcrossed on a C57BL/6 background (>10 generations) have been described previously.[32, 34] To generate endothelial *Bambi* knock-out mice, *Tie2-Cre* [Jackson Laboratory no 008863 B6.Cg-Tg(Tekcre)1Ywa/J] males were crossed with *Bambi*^{flox/flox} female mice. *Bambi*^{flox/flox} *Tie2-Cre*⁺ males were further bred with *Bambi*^{flox/flox} female mice to generate *Bambi*^{flox/flox} *Tie2-Cre*⁺ mice. Genotyping of *Bambi*^{flox/flox} and *Bambi*^{/-} have been previously described.[32, 34]. For the detection of the *Cre* allele the following primers (FW: GCCTGCATTACCGGTCGATGCAACGA and R: GTGGCAGATGGCGCGGCAACA CCATT) were used.

Prostacyclin and nitric oxide plasma levels

Prostacyclin plasma levels were determined by measuring the stable analogue 6-keto-PGF_{1 α} by ELISA according to the manufacturer's specifications (Cayman Chemical). Plasma nitrite and nitrate levels were determined by Griess colorimetric assay according to the manufacturer's instructions (Cayman Chemical).

Isolation of MLEC and MBEC

Primary mouse lung endothelial cells (MLEC) were isolated as previously described with modifications.[37] Briefly, minced lungs from <3 week-old mice were digested with 0.2% collagenase type II (Invitrogen). Cells were sieved (70 µm cell strainer, Corning) and centrifuged at 350xg for 5 min and resuspended in 1 ml of isolation medium. EC were selected by immunosorting using sheep anti-rat Dynabeads (Invitrogen) precoated with rat anti-mouse platelet endothelial cell adhesion molecule 1 (PECAM-1) antibody (MEC 13.3, BD Biosciences). Bound EC were released from the beads using trypsin digestion. Cells were cultured in EGM-2 MV media (Lonza) in 6 well plates (1 well/mouse) precoated with 1x Attachment Factor Protein (Invitrogen). Purity of the cells were assessed by flow cytometry using rat anti-mouse CD54-Alexa 488, rat anti-mouse CD31-PE/Cy7, rat anti-mouse CD102-Alexa 647 and corresponding control IgG antibodies (Biolegend). MLEC (purity 60-90%) were passaged 2-8 times and used for all experiments.

Primary mouse brain endothelial cells (MBEC) were isolated as previously described.[38] Briefly, brains from 5 sex and age matched *Bambi^{/-}* and *Bambi^{+/+}* mice were rolled on a sterile filter paper to remove meninges. Brains were transferred into hand homogenizer with isolation medium: HBSS (Invitrogen) supplemented with 10mM HEPES, 1X penicillin-Streptomycin (Sigma) and 0.5% BSA (First Link). Brain microvessels were obtained by series of centrifugation in 22% BSA, and digested in 0.5 mg/ml collagenase/dispase (Roche) and 0.5 mg/ml collagenase (Invitrogen) for 60-90 min at 37°C. Cells were centrifuged, washed and resuspended in EGM-2 media supplemented with growth factors (CC-4176; Lonza) and 5 µg/ml puromycin (first 48h only). Cells were grown to confluency in fibronectin (Sigma) coated wells.

Western blot

Whole cell protein lysates were prepared from lungs, MLEC and MBEC with RIPA buffer (Sigma) supplemented with protease and phosphatase inhibitors (cOmplete, mini and PhosSTOP from Roche). Protein concentrations were determined with BCA protein assay (Thermo Fisher Scientific). Immunoblotting of lysates was performed using reducing conditions (except for TFPI expression levels) with 4-12% NuPAGE pre-cast gels and transfer units (Invitrogen). Blocked membranes were incubated overnight at 4°C with the following primary antibodies: mouse anti-porcine GAPDH rabbit anti-mouse eNOS and peNOS (Novus Biological), (Santa Cruz Biotechnology), rat anti-mouse PECAM-1 (BD Biosciences), rat anti-mouse ICAM-1 (Biolegend), goat anti-mouse thrombomodulin (R&D), goat anti-mouse TFPI (R&D), rabbit anti-human fibrinogen α (Santa Cruz Biotechnology). Detection and quantification of chemiluminescence intensity were quantified by using Chemidoc[™] imaging system and Image Lab 5.2.1 software (Biorad). Protein levels were quantified and normalised against loading controls (GAPDH).

APC generation assay

APC generation assays were carried out as previously described.[39] MLEC from *Bambi^{-/-}* mice and wild-type littermates were isolated in parallel and grown to confluency. Cells were washed twice in HBSS and once in assay buffer (20mM Tris, 100mM NaCl, 1mM CaCl₂, 0.1% BSA pH 7.5) prior addition of 100nM recombinant human protein C (see below) together with 2nM human thrombin (Enzyme Research

Laboratories). APC activation occurred at 37°C and reactions were stopped (0-60 min) by addition of hirudin (100nM; Sigma). Control cells were preincubated with 50nM goat anti-thrombomodulin (R&D) antibody for 30 min to block endogenous thrombomodulin and washed 3 times before addition of protein C. APC was quantified by cleavage of the chromogenic substrate S-2366 (0.5mM; Chromogenix). The rate of cleavage was followed for 20 min at 37°C using an ELx808 plate reader (Perkin Elmer) and the concentration of APC extrapolated from a standard curve of purified human APC (Haematologic Technologies Inc.). Control experiments lacking thrombin or protein C were performed to demonstrate the specificity of the substrate cleavage.

Protein C expression and purification

Human protein C was expressed using stably transfected HEK293 cells, as previously described.[40] Vitamin K was added to culture medium to enable γ-carboxylation. Conditioned media containing protein C was harvested and concentrated ~20 fold by tangential flow filtration (Millipore). Protein C was purified by barium citrate precipitation, according to a previously described protocol,[41] followed by anion-exchange chromatography. For this, the partially purified protein C was applied on a HiTrap DEAE fast flow column (5 ml, GE healthcare) equilibrated with TBS. After washing with the same buffer, protein C was eluted with a 35 ml linear CaCl₂ gradient (0-30mM). Fractions were analyzed using 4-15% SDS-PAGE under non-reducing conditions and those containing pure protein C were pooled and dialyzed in TBS, 3mM CaCl₂. The pure protein C was concentrated, as required, and the protein C concentration determined by absorbance at 280nm using extinction coefficient (E1%, 1cm) of 14.5.[42]

Calibrated automated thrombography (CAT)

Thrombin generation was assessed by calibrated automated thrombography (CAT) using a Fluoroskan Ascent FL plate reader (Thermo) in combination with Thrombinoscope software (Synapse BV) as described previously.[13, 43] Briefly, the generation of thrombin was quantified in human plasma (80 µl per well) supplemented with 4µM phospholipid vesicles in the presence and absence of 10nM recombinant mouse thrombomodulin (R&D) and 10-100nM goat anti-mouse thrombomodulin antibody (R&D). Coagulation was initiated with 4pM TF (Dade

Innovin, Dade Behring) and 16.6mM $CaCl_2$. Contact activation coagulation was inhibited by adding corn trypsin inhibitor (40 μ g/ml plasma) and thrombin generation quantified by adding 0.42mM of Z-GlyArg-AMC-HCl (Bachem).

FXa inhibition assay by TFPI

FXa (0.5nM; Enzyme Research Laboratories) activity was monitored by the cleavage of the chromogenic substrate S-2765 (200 μ M; Chromogenix) for 40 min at 25°C in the presence or absence of 8nM recombinant murine TFPI (mTFPI), 40nM polyclonal goat anti-mouse TFPI (R&D) in the presence of 25 μ M phospohlipids and 5 mM CaCl₂, as described previously.[12, 13]

Intravital microscopy

The laser induced thrombosis model was performed as previously described using a VIVO platform (3i).[34] Briefly, mice were anaesthetized with ketamine (75mg/kg) and medetomidine (1mg/kg) and given additional ketamine (7.5mg/kg) every 40 minutes to maintain anaesthesia. Platelets, neutrophil or fibrin were visualized by injecting Dy-Light 488 conjugated rat anti-mouse GPIbß (0.15µg/g;Emfret), PE conjugated rat anti-mouse Ly6G (0.15µg/g; BD Biosciences) or Alexa 647 conjugated fibrinogen (5% total fibrinogen; Invitrogen), respectively, 15 min prior to the laser injury via a cannula placed in the jugular vein. Control experiments using labelled control IgG/proteins were carried out to ensure detection of specific fluorescence in Alexa-488, PE- or Alexa-647 channels. Goat anti-mouse thrombomodulin or anti-mouse TFPI antibodies or goat IgG (R&D; 1.9µg/g) were injected together with reagents labelling platelets and fibrin. When indicated, hirudin (Refludan, CSL Behring GmbH, 15µg/g) was injected into mice after 4 or 5 thrombi. The vessel wall injury was performed by a pulse laser (Ablate!, 3i) focused through a 63X water-immersion objective (65-75% intensity, 5-15 pulses). Image analysis was performed as previously described to determine the median integrated fluorescence intensity over time; differences in platelet or fibrin accumulation between genotypes was assessed by comparing the median values of area under the curves for Thrombus fluorescence at 490nm and 647nm, respectively, vs time. [34] embolization events were assessed by counting the number of emboli (>25% maximum thrombus size) detaching from the injury site/thrombus over time. Genotypes of the mice were blinded to the operator during data acquisition and analysis.

Statistical analysis

Unless otherwise indicated, results are presented as mean \pm SEM from n≥3 mice per experimental group and analyzed using GraphPad Prism (v7). Statistical analysis was performed using unpaired student *t* test with Welsch correction when applicable for parametric comparisons or Mann Whitney test for non-parametric comparisons.

Results

Bambi^{/-} mice have normal vasodilator function of the endothelium

We previously demonstrated that BAMBI in the vessel wall (rather than the hematopoietic compartment) is important for thrombus stability.[34] As BAMBI is highly expressed in EC, we hypothesized that loss of BAMBI function may alter the hemostatic function of the endothelium. Levels of the stable derivative of prostacyclin, 6-keto-PGF_{1α}, were similar in plasma from *Bambi^{-/-}* and *Bambi^{+/+}* mice, and no differences in plasma nitrate and nitrite levels were detected, indicating normal nitric oxide production (Fig. S1A-B). Moreover, there was no difference in levels of phosphorylated eNOS in lung extracts from *Bambi*-deficient mice (Fig. S1C). Together, these results suggest that neither prostacyclin nor nitric oxide levels influence the thrombus stability in *Bambi*-deficient mice.

Bambi deficiency does not alter neutrophil recruitment to the endothelium following laser injury

Similar to our previous results,[34] *Bambi^{/-}* mice formed thrombi, revealed by the normal time to maximal thrombus and the maximal thrombus size (Fig. S2A-B). However, in stark contrast to wild-type littermates, they were unable to sustain the thrombi at the site of injury (Movie S1, Fig. 1A-D). The overall extent of thrombus formation (i.e. area under the curve) was reduced (Fig. 1A-C; Fig. S2C) and the number of embolization events (excluding normal shedding observed in this laser injury model) were significantly increased in *Bambi^{/-}* mice compared to *Bambi^{+/+}* littermates (Fig. 1D).

In the laser injury thrombosis model, neutrophils have been reported to interact with the activated endothelium and augment thrombus formation.[2] In this model, blocking endothelial intercellular adhesion molecule 1 (ICAM-1) prevents neutrophil recruitment and consequently greatly reduces both platelet and fibrin accumulation after the vascular injury.[2] We therefore examined neutrophil accumulation in *Bambī^{/-}* mice using the laser-induced thrombosis model. Interestingly, there was no difference in the kinetics of neutrophil recruitment after the injury (Fig. 1E) or in the peak neutrophil accumulation (maximal IFI neutrophils; data not shown).

Consistent with these *in vivo* observations, MLEC isolated from *Bambi¹⁻* mice displayed broadly similar expression levels of ICAM-1 (and also other endothelial cell adhesion molecules, PECAM-1 and ICAM-2) (Fig. 2), suggesting that neutrophils bind normally to the activated endothelium after laser injury and do not impact upon thrombus stability in *Bambi*-deficient mice.

Thrombus instability in Bambi^{/-} mice is accompanied by lack of fibrin accumulation

We next hypothesized that *Bambi* deficiency may alter the anticoagulant function of the endothelium, and therefore examined whether thrombin generation (as measured by fluorescent fibrin deposition) might be impaired in *Bambi*-deficient mice. Following laser-induced injury, thrombus instability in *Bambi*^{-/-} mice, observed by decreased thrombus formation over time (Fig. 3A-C) and increased embolization events (Fig. 3D), was accompanied by a large reduction (~80%) in fibrin accumulation over time (Fig. 3E; Movie S2). This was not due to differences in endogenous fibrinogen levels as *Bambi*^{-/-} mice exhibited normal plasma fibrinogen concentration (Fig. S3).

To ascertain whether the reduced fibrin accumulation was due to inefficient thrombin generation we injected the potent thrombin inhibitor, hirudin, into mice prior to laser-induced thrombosis. As previously shown in this model,[3, 44, 45] injection of hirudin in wild-type (*Bambi*^{+/+}) mice led to a reduction of platelet accumulation (Fig. 4A-C). Interestingly, inhibiting thrombin generation with hirudin in *Bambi*^{+/+} mice appeared to phenocopy the thrombus instability of *Bambi*^{-/-} mice (Fig. 4D; Movie S3). Platelet thrombi formed initially (i.e. there was no difference in maximal platelet thrombus size observed in *Bambi*^{+/+} mice in the presence of hirudin, data not shown) but due to the lack of fibrin accumulation thrombi were unstable. Interestingly, we saw no discernible effect of hirudin upon thrombus formation in *Bambi*^{-/-} mice (Fig. 4B-D),

supporting the contention that impaired fibrin deposition during thrombus formation is likely caused by reduced thrombin generation in *Bambi*-deficient mice.

Tissue-specific deletion of BAMBI in the endothelium leads to thrombus instability and lack of fibrin generation

Using chimeric *Bambi^{-/-}* mice, we previously demonstrated that BAMBI in the vessel wall, rather than in the hematopoietic compartment, influenced thrombus formation.[34] To more specifically explore the role of endothelial BAMBI (rather than other extravascular cells) in thrombus stability, we generated endothelium-specific *Bambi*-deficient mice (*Bambi*^{flox/flox} *Tie2-Cre*⁺) using the Cre/Lox system and previously characterized *Tie2-Cre* mice (Fig. S4 A-C).[46-48] Unlike a proportion of *Bambi*^{-/-} mice,[34] all *Bambi*^{flox/flox} *Tie2-Cre*⁺ mice were viable and pups were similar in weight when compared to *Bambi*^{flox/flox} littermates. To evaluate the role of endothelial BAMBI in hemostasis, we performed tail bleeding assays. Whereas *Bambi*^{flox/flox} *Tie2-Cre*⁺ mice, this was not significant (data not shown). Moreover, there was no significant difference in the extent of blood loss between the mice (Fig. S4D).

To explore the role of endothelial BAMBI in thrombus formation, we performed the laser-induced thrombosis model in *Bambi^{flox/flox} Tie2-Cre*⁺ mice. There was no difference in platelet accumulation between *Bambi^{flox/flox} Tie2-Cre*⁺ mice and *Bambi^{flox/flox}* mice (Fig. 5A-B), but there was a significant increase in thrombus embolization (Fig. 5C; Movie S4). Thrombus instability was also accompanied with a decrease in fibrin accumulation (Fig. 5D), as observed for *Bambi^{/-}* mice (Fig. 3D). Collectively, these results suggest that deficiency of endothelial BAMBI influences both fibrin accumulation and thrombus stability after laser injury.

Bambi⁻⁻ mice exhibit increased TFPI and thrombomodulin expression levels

Our results suggest that *Bambi*-deficient EC are responsible for the reduced propensity to generate fibrin after vascular injury. We hypothesized that the thromboprotective phenotype observed in *Bambi*-deficient mice could be due to increased anticoagulant function of the endothelium - more specifically due to elevated TFPI function and/or APC generation. Although no significant differences in *Tfpi, Procr* or *Thbd* mRNA levels (corresponding to TFPI, EPCR and thrombomodulin genes, respectively) were detected in lungs or MLEC from *Bambi*^{-/-}

compared to *Bambi*^{+/+} mice (data not shown), Western blot analysis of lung extracts revealed that both total TFPI and thrombomodulin levels were 60-80% increased in *Bambi*^{-/-} mice compared to *Bambi*^{+/+} mice (Fig. 6A-B). Elevated thrombomodulin was also detected in MLEC and MBEC isolated from *Bambi*^{-/-} mice compared to *Bambi*^{+/+} mice (Fig. S5). Thrombomodulin binds thrombin with high affinity and, in so doing, facilitates protein C activation. To functionally assess the influence of elevated thrombomodulin levels on *Bambi*^{-/-} MLEC, we performed APC generation assays. Significant increase in APC generation after 30 and 60 min was detected in *Bambi*^{-/-} MLEC compared to *Bambi*^{+/+} MLEC (Fig. 6C). The specificity of the assay for thrombomodulin was confirmed using an inhibitory anti-thrombomodulin polyclonal antibody.[39] As shown in Fig. 6C, blocking thrombomodulin decreased APC generation on both *Bambi*^{-/-} and *Bambi*^{+/+} MLEC by ~90%. These data demonstrate that elevated levels of thrombomodulin on EC from *Bambi*^{-/-} mice can lead to increased propensity to generate APC.

Blocking TFPI and thrombomodulin function restores fibrin accumulation and thrombus stability in Bambi⁷⁻ mice

To investigate the influence of elevated TFPI and thrombomodulin in *Bambi*-deficient mice upon fibrin accumulation and thrombus stability *in vivo*, we performed the laser-induced thrombosis model under conditions where each endogenous anticoagulant protein was blocked using inhibitory polyclonal anti-thrombomodulin and anti-TFPI antibodies. Blocking thrombomodulin inhibited APC generation on cells *in vitro* (Figure 6C), and also using calibrated automated thrombography in the presence of recombinant murine soluble thrombomodulin (Fig. S6A). The anti-TFPI antibody inhibited murine TFPI function in FXa inhibition assays (Fig. S6B).

Similar to earlier observations (Figures 1,3,4), *Bambi^{/-}* mice (injected with control goat IgG) exhibited a significant reduction in platelet accumulation over time (Fig. 7A-B) and increased number of emboli (Fig. 7C) compared to wild-type animals (also injected with control goat IgG). As before, fibrin accumulation over time in *Bambi^{/-}* mice was also significantly attenuated (Fig. 7A;Dii and Movie S5).

In wild-type mice, inhibition of thrombomodulin alone had no significant effect upon platelet thrombus formation (Fig. 7A, Bi), the frequency of embolization (Fig. 7Ci), or fibrin accumulation after laser injury (Fig. 7Di; Movie S6). In *Bambi^{/-}* mice, blocking thrombomodulin induced an increase in platelet accumulation (Fig. 7Bi), reduced

embolization (Fig. 7Cii), and increased fibrin accumulation (Fig. 7Dii; Movie S5) although it did not reach statistical significance.

Although blocking TFPI in wild-type mice had no effect upon platelet thrombi or embolization (Fig. 7Bii, Ci), this caused a significant increase in fibrin deposition (Fig. 7Di; Movie S6), consistent with the primary role of TF in initiating coagulation in this model.[2, 44, 45] A very similar effect was also seen in *Bambi^{/-}* mice (Fig. 7Dii). Interestingly, simultaneous inhibition of both thrombomodulin and TFPI function in *Bambi^{/-}* mice significantly reduced embolization to similar levels to those observed in wild-type mice (Fig. 7Cii; Movies S5 and S6). Moreover, fibrin deposition was also normalized (Fig. 7A;Dii). Collectively, these results suggest that loss of BAMBI influences fibrin formation and thrombus stability by altering the levels of thrombomodulin and TFPI on the endothelial surface.

Discussion

We previously reported that lack of BAMBI reduces thrombus formation/stability in two different *in vivo* models of thrombosis.[34] Using endothelial-specific *Bambi*-knockout mice and intravital imaging, we here confirm a role for endothelial BAMBI in the formation of a stable thrombus after vascular injury. Further, we show that the thrombus formation/stability defect in *Bambi*-deficient mice is associated with defective fibrin accumulation. Our data also identify the contributions of elevated TFPI and thrombomodulin to the decreased thrombin generation and increased embolization seen in *Bambi*^{-/-} mice.

Formation of a stable thrombus after vascular injury requires the concerted action of vessel wall components (e.g. extravascular TF, subendothelial matrix and activated EC), the coagulation system, platelets, and as recently demonstrated, other cells including red blood cells and neutrophils.[2, 5] The importance of neutrophil accumulation mediated by lymphocyte function-associated antigen 1 (LFA-1) expressed on neutrophils and ICAM-1 expressed on EC in the laser-induced thrombosis model of the cremaster arterioles has recently been demonstrated.[2, 49] Using the same approach as Darbousset *et al*,[2] we confirm the recruitment of neutrophils after the vascular injury in this thrombosis model, however, we detected normal accumulation of neutrophils/neutrophil-derived particles in the laser-induced thrombi of *Bambi*^{+/+} and *Bambi*^{-/-} mice (Figure 1). This suggested that EC present

ICAM-1 normally after activation, [50] and consistent with this, no difference in the expression of several endothelial cell markers was detected in Bambi^{/-} MLEC (Fig. 2). Once bound, neutrophils can enhance coagulation and promote thrombus formation.[49] Conceivably, recruited Bambi^{/-} neutrophils may be defective in their activation leading to reduced thrombin generation and fibrin. However, this was excluded as the hemostatic defect in Bambi/- mice was phenocopied by the endothelial cell-specific deletion of Bambi (Figure 5) and was also present in chimeric Bambi/- mice reconstituted with wild-type bone marrow cells.[34] Similarly, although one cannot formally exclude a possible role for elevated fibrinolysis in thrombus instability caused by alterations in regulators associated with this pathway (e.g. TAFI, PAI-1, tPA), based on the literature it is unlikely they could be major contributors to the phenotype that we observed in Bambi^{/-} mice. Indeed, full deficiencies in these markers have not always been reported to protect against thrombosis depending of the model chosen in the study (arterial or venous thrombosis) and the vascular bed (carotid, mesenterium, femoral).[51-54] Moreover, in order for fibrinolysis to occur, fibrin needs to be deposited first at the site of injury before fibrinolysis is efficiently activated.

We next evaluated the influence of anticoagulant pathways in thrombus formation and stability in *Bambi^{/-}* mice. In the laser-induced thrombosis model, endothelial activation results in increased ICAM-1 and LAMP-1 presentation.[50, 55] Platelets (and leukocytes) are recruited at the site of injury, become activated by locally generated thrombin, which creates a core of activated platelets overlaid by a shell of P-selectin negative platelets.[3, 8] Fibrin is associated with the core of tightly packed P-selectin positive platelets and extends into the vasculature [3, 8] but can also be detected away from the vascular injury on the activated endothelium itself.[6] Strikingly, Bambi^{/-} and Bambi^{flox/flox} Tie2-Cre⁺ mice were unable to efficiently accumulate fibrin or to sustain thrombus formation after vascular injury (Figs. 3E and 5D). This may be unsurprising given the role of fibrin in thrombus stability.[56, 57] However, it is also important to note that fibrin accumulation in this model can occur without appreciable platelet accumulation, as observed for example in $Par4^{-1}$ mice.[45] Another group has also shown that platelet accumulation at the site of vascular injury is not a prerequisite for fibrin deposition,[6] supporting the contention that altered platelet accumulation is unlikely to be responsible for the reduced ability of *Bambi^{/-}* mice to generate fibrin.

Despite the clear defect in fibrin accumulation and increased thrombus instability, platelet accumulation over time after the vascular injury in *Bambi^{flox/flox} Tie2-Cre*⁺ mice was not statistically different from *Bambi^{flox/flox}* mice (Figure 5B) suggesting that thrombi are more likely reforming in *Bambi^{flox/flox} Tie2-Cre*⁺ mice after embolization. Interestingly, in contrast to *Bambi^{rl-}* mice, *Bambi^{flox/flox} Tie2-Cre*⁺ mice had also normal hemostasis/tail bleeding (Fig. S4), exhibited no difference in weight compared to littermates and were all viable. Our data therefore point to an important role for endothelial BAMBI in fibrin deposition/thrombus stability, but imply that the phenotypic differences observed between the constitutive and conditional *Bambi* knockout mice are manifest through roles for BAMBI in cellular compartments other than the endothelium.

Injection of hirudin in *Bambi*^{+/+} mice had minimal effect on the maximal platelet thrombus size (i.e. platelet accumulation) reached within 40-60 sec post injury (data not shown), but had significant effect upon overall thrombus formation (Fig. 4C) due to the reduction of fibrin deposition, which was associated with decreased thrombus stability (Fig. 4D). These effects of hirudin on thrombus formation are consistent with several reports,[3, 4, 45, 58] as well as its minimal effect on maximal thrombus size.[58] Interestingly, the kinetics of thrombus formation in hirudin-injected *Bambi*^{+/+} mice closely resembled those observed in *Bambi*^{-/-} mice. Moreover, injection of hirudin into *Bambi*^{-/-} mice did not further diminish thrombus formation or further increase the number of emboli. These results strongly suggest that the lack of fibrin accumulation in *Bambi*^{-/-} mice is the major cause of the thrombus instability, and that the reason for reduced fibrin in the thrombus is most likely due to lower levels of thrombin generated at the site of injury would also impact upon platelet activation and exacerbate the thrombus instability phenotype in *Bambi*^{-/-} mice (Fig. S7).

The increase in thrombomodulin levels on *Bambi^{/-}* MLEC was associated with increased ability to generate APC (Fig. 6). *In vivo* inhibition of thrombomodulin in *Bambi^{/-}* mice moderately improved fibrin deposition, platelet accumulation and thrombus stability (Fig. 7Bi;Cii;Dii). TFPI blockade in *Bambi^{/-}* mice had a similar influence upon platelet accumulation and thrombus stability as blocking thrombomodulin (Fig. 7Bii, Cii). However, fibrin accumulation was significantly increased (Fig. 7Dii). Interestingly, inhibition of thrombomodulin in *Bambi^{+/+}* had little effect on fibrin accumulation, whereas TFPI inhibition led to a dramatic increase in

fibrin (Fig. 7Di). Our results therefore suggest that the importance of TFPI in regulating coagulation in the laser injury thrombosis model exceeds that of thrombomodulin. This is consistent with the well-documented role of TF in this model.[2, 44, 45] This may also be compatible with the role of thrombomodulin in limiting the spread of the hemostatic plug, rather than diminishing thrombin generation within the core of the thrombus.

Shortening of vessel occlusion times and increased thrombus volumes have been reported in mice variably (rather than completely) deficient in TFPI and thrombomodulin using different thrombosis models,[59-63] however, this is the first report evaluating the importance of these proteins in the laser-induced thrombosis model of the cremaster muscle arterioles. Ellery *et al* showed no effect upon fibrin accumulation in *Tfpi*^{-/-} *Par4*^{-/-} compared to *Par4*^{-/-} mice using a venous electrolytic injury model.[63] There was also no discernible contribution of platelet TFPI for fibrin generation in this model [62] unless combined with FVIII deficiency.[61] As suggested by Ellery *et al*,[63] the electrolytic injury model may not be particularly sensitive to changes in endothelial TFPI levels due to the nature of the injury, which may be less dependent upon TF for fibrin deposition than in laser-induced thrombus formation (Fig. 7D).

Inhibition of thrombomodulin or TFPI alone in *Bambi^{7/-}* mice was not sufficient to restore thrombus stability, whereas combined targeting of these anticoagulant proteins in these mice led to further increase in fibrin deposition in addition to a decrease in embolization events (Fig. 7Ciii,Dii). Mechanistically, elevated TFPI levels on the endothelium could contribute to inefficient thrombin generation, particularly in the settings of mild injuries that are dependent upon TF. Once coagulation is allowed to proceed, elevated thrombomodulin levels promoting protein C activation could further accentuate it, leading to lack of fibrin accumulation in *Bambi^{7/-}* mice. The reason why blocking thrombomodulin alone did not exert a stronger effect may be linked to the dependency of this pathway upon thrombin. When thrombomodulin alone is inhibited, the elevated TFPI levels do not permit sufficient thrombin generation to appreciably activate this pathway. Only when TFPI is inhibited does this provide increased thrombin that enable the contribution of the protein C pathway to be detected in *Bambi^{7/-}* mice. Together, these data suggest that reduced fibrin deposition after injury in *Bambi*-deficient mice is linked to both higher levels of

thrombomodulin and TFPI on the endothelial cell surface. Of note, we did not detect any difference in expression levels of plasma TFPI (TFPI γ) in *Bambi^{'-}* mice.

In conclusion, we demonstrate that BAMBI influences the phenotype of the endothelium, and deficiency from these cells precipitates thrombus instability due to reduced fibrin deposition. Our data suggest that BAMBI mediates its effect via modulation of the natural anticoagulant function of the endothelium. As we found no discernible/major differences in *Tfpi* or *Thbd* mRNA levels in *Bambi*⁷⁻ mice, we hypothesize that BAMBI may influence cell surface thrombomodulin and TFPI levels through modulation of cell surface shedding and/or internalization, which is the focus of on-going studies. It still remains unclear how BAMBI exerts its function at a molecular level, whether via TGF β /BMP/activin-dependent or -independent mechanisms. Understanding how and when BAMBI interacts with both extracellular and intracellular binding partners will help define its physiological role and how this influences endothelial function.

Addendum

James TB Crawley designed the research and wrote the paper; Argita Zalli, James H. Monkman, and Anastasis Petri performed experiments and analyzed data; David A. Lane designed the research and revised the manuscript; Josefin Ahnström designed the research, analysed data and revised the manuscript; Isabelle I. Salles-Crawley designed and performed experiments, analyzed data and wrote the paper.

Acknowledgements

The authors thank all staff from Central Biomedical Services at Imperial College. We would like to thank Professor A.M. Randi and Dr G.M. Birdsey (both Imperial College London) for providing *Tie2-Cre* mice, their assistance in the breeding and genotyping of these mice and Dr M.N O'Connor (University College London) for her help in the isolation of EC from mouse brains.

This work was supported by the British Heart Foundation grants FS/10/004/28165, PG/14/90/31219, PG/17/42/33039 and FS/12/60/29874.

Disclosure of Conflict of Interests

The authors state that they have no conflict of interest.

References

1 Falati S, Gross P, Merrill-Skoloff G, Furie BC, Furie B. Real-time in vivo imaging of platelets, tissue factor and fibrin during arterial thrombus formation in the mouse. *Nature Medicine*. 2002; **8**: 1175-81.

2 Darbousset R, Thomas GM, Mezouar S, Frere C, Bonier R, Mackman N, Renne T, Dignat-George F, Dubois C, Panicot-Dubois L. Tissue factor-positive neutrophils bind to injured endothelial wall and initiate thrombus formation. *Blood.* 2012; **120**: 2133-43. 10.1182/blood-2012-06-437772.

3 Stalker TJ, Traxler EA, Wu J, Wannemacher KM, Cermignano SL, Voronov R, Diamond SL, Brass LF. Hierarchical organization in the hemostatic response and its relationship to the platelet-signaling network. *Blood.* 2013; **121**: 1875-85. 10.1182/blood-2012-09-457739.

4 Hechler B, Nonne C, Eckly A, Magnenat S, Rinckel JY, Denis CV, Freund M, Cazenave JP, Lanza F, Gachet C. Arterial thrombosis: relevance of a model with two levels of severity assessed by histologic, ultrastructural and functional characterization. *J Thromb Haemost.* 2010; **8**: 173-84. 10.1111/j.1538-7836.2009.03666.x.

5 Walton BL, Lehmann M, Skorczewski T, Holle LA, Beckman JD, Cribb JA, Mooberry MJ, Wufsus AR, Cooley BC, Homeister JW, Pawlinski R, Falvo MR, Key NS, Fogelson AL, Neeves KB, Wolberg AS. Elevated hematocrit enhances platelet accumulation following vascular injury. *Blood*. 2017; **129**: 2537-46. 10.1182/blood-2016-10-746479.

6 Ivanciu L, Krishnaswamy S, Camire RM. New insights into the spatiotemporal localization of prothrombinase in vivo. *Blood.* 2014; **124**: 1705-14. 10.1182/blood-2014-03-565010.

7 de Witt SM, Swieringa F, Cavill R, Lamers MM, van Kruchten R, Mastenbroek T, Baaten C, Coort S, Pugh N, Schulz A, Scharrer I, Jurk K, Zieger B, Clemetson KJ, Farndale RW, Heemskerk JW, Cosemans JM. Identification of platelet function defects by multiparameter assessment of thrombus formation. *Nat Commun.* 2014; **5**: 4257. 10.1038/ncomms5257.

8 Stalker TJ, Welsh JD, Tomaiuolo M, Wu J, Colace TV, Diamond SL, Brass LF. A systems approach to hemostasis: 3. Thrombus consolidation regulates intrathrombus solute transport and local thrombin activity. *Blood.* 2014; **124**: 1824-31. 10.1182/blood-2014-01-550319.

9 Welsh JD, Stalker TJ, Voronov R, Muthard RW, Tomaiuolo M, Diamond SL, Brass LF. A systems approach to hemostasis: 1. The interdependence of thrombus architecture and agonist movements in the gaps between platelets. *Blood.* 2014; **124**: 1808-15. 10.1182/blood-2014-01-550335.

10 Cosemans JM, Angelillo-Scherrer A, Mattheij NJ, Heemskerk JW. The effects of arterial flow on platelet activation, thrombus growth, and stabilization. *Cardiovasc Res.* 2013; **99**: 342-52. 10.1093/cvr/cvt110.

11 Crawley JT, Lane DA. The haemostatic role of tissue factor pathway inhibitor. *Arterioscler Thromb Vasc Biol.* 2008; **28**: 233-42. 10.1161/ATVBAHA.107.141606.

12 Reglinska-Matveyev N, Andersson HM, Rezende SM, Dahlback B, Crawley JT, Lane DA, Ahnstrom J. TFPI cofactor function of protein S: essential role of the protein S SHBG-like domain. *Blood.* 2014; **123**: 3979-87. 10.1182/blood-2014-01-551812.

Ahnstrom J, Andersson HM, Hockey V, Meng Y, McKinnon TA, Hamuro T, Crawley JT, Lane DA. Identification of functionally important residues in TFPI Kunitz domain 3 required for the enhancement of its activity by protein S. *Blood*. 2012; **120**: 5059-62. 10.1182/blood-2012-05-432005.

14 Maroney SA, Hansen KG, Mast AE. Cellular expression and biological activities of alternatively spliced forms of tissue factor pathway inhibitor. *Curr Opin Hematol.* 2013; **20**: 403-9. 10.1097/MOH.0b013e3283634412.

15 Maroney SA, Ellery PE, Wood JP, Ferrel JP, Martinez ND, Mast AE. Comparison of the inhibitory activities of human tissue factor pathway inhibitor (TFPI)alpha and TFPIbeta. *J Thromb Haemost.* 2013; **11**: 911-8. 10.1111/jth.12188. 16 Maroney SA, Ferrel JP, Collins ML, Mast AE. Tissue factor pathway inhibitor-gamma is an active alternatively spliced form of tissue factor pathway inhibitor present in mice but not in humans. *J Thromb Haemost.* 2008; **6**: 1344-51. 10.1111/j.1538-7836.2008.03033.x.

17 Maroney SA, Ferrel JP, Pan S, White TA, Simari RD, McVey JH, Mast AE. Temporal expression of alternatively spliced forms of tissue factor pathway inhibitor in mice. *J Thromb Haemost.* 2009; **7**: 1106-13. 10.1111/j.1538-7836.2009.03454.x.

18 Girard TJ, Grunz K, Lasky NM, Malone JP, Broze GJ, Jr. Re-evaluation of mouse tissue factor pathway inhibitor and comparison of mouse and human tissue factor pathway inhibitor physiology. *J Thromb Haemost*. 2018; **16**: 2246-57. 10.1111/jth.14288.

19 Conway EM. Thrombomodulin and its role in inflammation. *Semin Immunopathol.* 2012; **34**: 107-25. 10.1007/s00281-011-0282-8.

20 Loghmani H, Conway EM. Exploring traditional and nontraditional roles for thrombomodulin. *Blood*. 2018; **132**: 148-58. 10.1182/blood-2017-12-768994.

21 Montes R, Puy C, Molina E, Hermida J. Is EPCR a multi-ligand receptor? Pros and cons. *Thromb Haemost*. 2012; **107**: 815-26. 10.1160/TH11-11-0766.

22 Stearns-Kurosawa DJ, Kurosawa S, Mollica JS, Ferrell GL, Esmon CT. The endothelial cell protein C receptor augments protein C activation by the thrombin-thrombomodulin complex. *Proc Natl Acad Sci U S A*. 1996; **93**: 10212-6.

Polderdijk SG, Adams TE, Ivanciu L, Camire RM, Baglin TP, Huntington JA. Design and characterization of an APC-specific serpin for the treatment of hemophilia. *Blood*. 2017; **129**: 105-13. 10.1182/blood-2016-05-718635.

Onichtchouk D, Chen YG, Dosch R, Gawantka V, Delius H, Massague J, Niehrs C. Silencing of TGF-beta signalling by the pseudoreceptor BAMBI. *Nature*. 1999; **401**: 480-5.

25 Yan X, Lin Z, Chen F, Zhao X, Chen H, Ning Y, Chen YG. Human BAMBI cooperates with Smad7 to inhibit transforming growth factor-beta signaling. *J Biol Chem.* 2009; **284**: 30097-104.

26 Seki E, De Minicis S, Osterreicher CH, Kluwe J, Osawa Y, Brenner DA, Schwabe RF. TLR4 enhances TGF-beta signaling and hepatic fibrosis. *Nat Med*. 2007; **13**: 1324-32.

27 Degen WG, Weterman MA, van Groningen JJ, Cornelissen IM, Lemmers JP, Agterbos MA, Geurts van Kessel A, Swart GW, Bloemers HP. Expression of nma, a novel gene, inversely correlates with the metastatic potential of human melanoma cell lines and xenografts. *Int J Cancer*. 1996; **65**: 460-5.

28 Grotewold L, Plum M, Dildrop R, Peters T, Ruther U. Bambi is coexpressed with Bmp-4 during mouse embryogenesis. *Mech Dev.* 2001; **100**: 327-30.

Tsang M, Kim R, de Caestecker MP, Kudoh T, Roberts AB, Dawid IB. Zebrafish nma is involved in TGFbeta family signaling. *Genesis*. 2000; **28**: 47-57.

30 Watkins NA, Gusnanto A, de Bono B, De S, Miranda-Saavedra D, Hardie DL, Angenent WG, Attwood AP, Ellis PD, Erber W, Foad NS, Garner SF, Isacke CM, Jolley J, Koch K, Macaulay IC, Morley SL, Rendon A, Rice KM, Taylor N, Thijssen-Timmer DC, Tijssen MR, van der Schoot CE, Wernisch L, Winzer T, Dudbridge F, Buckley CD, Langford CF, Teichmann S, Gottgens B, Ouwehand WH. A HaemAtlas: characterizing gene expression in differentiated human blood cells. *Blood*. 2009; **113**: e1-9.

O'Connor MN, Salles, II, Cvejic A, Watkins NA, Walker A, Garner SF, Jones CI, Macaulay IC, Steward M, Zwaginga JJ, Bray SL, Dudbridge F, de Bono B, Goodall AH, Deckmyn H, Stemple DL, Ouwehand WH. Functional genomics in zebrafish permits rapid characterization of novel platelet membrane proteins. *Blood*. 2009; **113**: 4754-62.

32 Chen J, Bush JO, Ovitt CE, Lan Y, Jiang R. The TGF-beta pseudoreceptor gene Bambi is dispensable for mouse embryonic development and postnatal survival. *Genesis*. 2007; **45**: 482-6.

33 Tramullas M, Lantero A, Diaz A, Morchon N, Merino D, Villar A, Buscher D, Merino R, Hurle JM, Izpisua-Belmonte JC, Hurle MA. BAMBI (bone morphogenetic protein and activin membrane-bound inhibitor) reveals the involvement of the transforming growth factorbeta family in pain modulation. *The Journal of neuroscience : the official journal of the Society for Neuroscience*. 2010; **30**: 1502-11. 10.1523/JNEUROSCI.2584-09.2010. 34 Salles C, II, Monkman JH, Ahnstrom J, Lane DA, Crawley JT. Vessel wall BAMBI contributes to hemostasis and thrombus stability. *Blood*. 2014; **123**: 2873-81. 10.1182/blood-2013-10-534024.

35 Guillot N, Kollins D, Gilbert V, Xavier S, Chen J, Gentle M, Reddy A, Bottinger E, Jiang R, Rastaldi MP, Corbelli A, Schlondorff D. BAMBI regulates angiogenesis and endothelial homeostasis through modulation of alternative TGFbeta signaling. *PLoS One*. 2012; **7**: e39406. 10.1371/journal.pone.0039406.

36 Fan Y, Li X, Xiao W, Fu J, Harris RC, Lindenmeyer M, Cohen CD, Guillot N, Baron MH, Wang N, Lee K, He JC, Schlondorff D, Chuang PY. BAMBI Elimination Enhances Alternative TGF-beta Signaling and Glomerular Dysfunction in Diabetic Mice. *Diabetes*. 2015; **64**: 2220-33. 10.2337/db14-1397.

37 Jin Y, Liu Y, Antonyak M, Peng X. Isolation and characterization of vascular endothelial cells from murine heart and lung. *Methods Mol Biol.* 2012; **843**: 147-54. 10.1007/978-1-61779-523-7_14.

Abbott NJ, Hughes CC, Revest PA, Greenwood J. Development and characterisation of a rat brain capillary endothelial culture: towards an in vitro blood-brain barrier. *J Cell Sci.* 1992; **103 (Pt 1)**: 23-37.

39 Greineder CF, Chacko AM, Zaytsev S, Zern BJ, Carnemolla R, Hood ED, Han J, Ding BS, Esmon CT, Muzykantov VR. Vascular immunotargeting to endothelial determinant ICAM-1 enables optimal partnering of recombinant scFv-thrombomodulin fusion with endogenous cofactor. *PLoS One*. 2013; **8**: e80110. 10.1371/journal.pone.0080110.

40 Andreou AP, Efthymiou M, Yu Y, Watts HR, Noormohamed FH, Ma D, Lane DA, Crawley JT. Protective effects of non-anticoagulant activated protein C variant (D36A/L38D/A39V) in a murine model of ischaemic stroke. *PLoS One*. 2015; **10**: e0122410. 10.1371/journal.pone.0122410.

41 Lorand L MK. Proteolytic enzymes in coagulation, fibrinolysis, and complement activation. Part A. Mammalian blood coagulation factors and inhibitors. *Methods Enzymol.* 1993; **222**: 1-559.

42 Kisiel WD, E.W. Protein C. *Methods Enzymol.* 1981; **80**: 320-32.

43 Ahnstrom J, Andersson HM, Canis K, Norstrom E, Yu Y, Dahlback B, Panico M, Morris HR, Crawley JT, Lane DA. Activated protein C cofactor function of protein S: a novel role for a gamma-carboxyglutamic acid residue. *Blood.* 2011; **117**: 6685-93. 10.1182/blood-2010-11-317099.

44 Dubois C, Panicot-Dubois L, Gainor JF, Furie BC, Furie B. Thrombin-initiated platelet activation in vivo is vWF independent during thrombus formation in a laser injury model. *J Clin Invest*. 2007; **117**: 953-60. 10.1172/JCI30537.

45 Vandendries ER, Hamilton JR, Coughlin SR, Furie B, Furie BC. Par4 is required for platelet thrombus propagation but not fibrin generation in a mouse model of thrombosis. *Proc Natl Acad Sci U S A*. 2007; **104**: 288-92. 10.1073/pnas.0610188104.

46 Constien R, Forde A, Liliensiek B, Grone HJ, Nawroth P, Hammerling G, Arnold B. Characterization of a novel EGFP reporter mouse to monitor Cre recombination as demonstrated by a Tie2 Cre mouse line. *Genesis*. 2001; **30**: 36-44.

47 de Lange WJ, Halabi CM, Beyer AM, Sigmund CD. Germ line activation of the Tie2 and SMMHC promoters causes noncell-specific deletion of floxed alleles. *Physiol Genomics*. 2008; **35**: 1-4. 10.1152/physiolgenomics.90284.2008.

48 Kisanuki YY, Hammer RE, Miyazaki J, Williams SC, Richardson JA, Yanagisawa M. Tie2-Cre transgenic mice: a new model for endothelial cell-lineage analysis in vivo. *Dev Biol.* 2001; **230**: 230-42. 10.1006/dbio.2000.0106.

49 Darbousset R, Delierneux C, Mezouar S, Hego A, Lecut C, Guillaumat I, Riederer MA, Evans RJ, Dignat-George F, Panicot-Dubois L, Oury C, Dubois C. P2X1 expressed on polymorphonuclear neutrophils and platelets is required for thrombosis in mice. *Blood*. 2014; **124**: 2575-85. 10.1182/blood-2014-04-571679.

50 Proulle V, Furie RA, Merrill-Skoloff G, Furie BC, Furie B. Platelets are required for enhanced activation of the endothelium and fibrinogen in a mouse thrombosis model of APS. *Blood.* 2014; **124**: 611-22. 10.1182/blood-2014-02-554980.

51 Declerck PJ, Gils A, De Taeye B. Use of mouse models to study plasminogen activator inhibitor-1. *Methods Enzymol.* 2011; **499**: 77-104. 10.1016/B978-0-12-386471-0.00005-5.

52 Morser J, Gabazza EC, Myles T, Leung LL. What has been learnt from the thrombinactivatable fibrinolysis inhibitor-deficient mouse? *J Thromb Haemost.* 2010; **8**: 868-76. 10.1111/j.1538-7836.2010.03787.x.

53 Nagashima M, Yin ZF, Zhao L, White K, Zhu Y, Lasky N, Halks-Miller M, Broze GJ, Jr., Fay WP, Morser J. Thrombin-activatable fibrinolysis inhibitor (TAFI) deficiency is compatible with murine life. *J Clin Invest*. 2002; **109**: 101-10. 10.1172/JCI12119.

54 Vercauteren E, Peeters M, Hoylaerts MF, Lijnen HR, Meijers JC, Declerck PJ, Gils A. The hyperfibrinolytic state of mice with combined thrombin-activatable fibrinolysis inhibitor (TAFI) and plasminogen activator inhibitor-1 gene deficiency is critically dependent on TAFI deficiency. *J Thromb Haemost.* 2012; **10**: 2555-62. 10.1111/jth.12036.

55 Atkinson BT, Jasuja R, Chen VM, Nandivada P, Furie B, Furie BC. Laser-induced endothelial cell activation supports fibrin formation. *Blood*. 2010; **116**: 4675-83. 10.1182/blood-2010-05-283986.

56 Wolberg AS. Determinants of fibrin formation, structure, and function. *Curr Opin Hematol.* 2012; **19**: 349-56. 10.1097/MOH.0b013e32835673c2.

57 Ni H, Denis CV, Subbarao S, Degen JL, Sato TN, Hynes RO, Wagner DD. Persistence of platelet thrombus formation in arterioles of mice lacking both von Willebrand factor and fibrinogen. *J Clin Invest*. 2000; **106**: 385-92. 10.1172/JCI9896.

58 Mangin P, Yap CL, Nonne C, Sturgeon SA, Goncalves I, Yuan Y, Schoenwaelder SM, Wright CE, Lanza F, Jackson SP. Thrombin overcomes the thrombosis defect associated with platelet GPVI/FcRgamma deficiency. *Blood.* 2006; **107**: 4346-53. 10.1182/blood-2005-10-4244.

59 Maroney SA, Cooley BC, Sood R, Weiler H, Mast AE. Combined tissue factor pathway inhibitor and thrombomodulin deficiency produces an augmented hypercoagulable state with tissue-specific fibrin deposition. *J Thromb Haemost.* 2008; **6**: 111-7. 10.1111/j.1538-7836.2007.02817.x.

60 Vicente CP, Weiler H, Di Cera E, Tollefsen DM. Thrombomodulin is required for the antithrombotic activity of thrombin mutant W215A/E217A in a mouse model of arterial thrombosis. *Thromb Res.* 2012; **130**: 646-8. 10.1016/j.thromres.2011.11.026.

Maroney SA, Cooley BC, Ferrel JP, Bonesho CE, Nielsen LV, Johansen PB, Hermit MB, Petersen LC, Mast AE. Absence of hematopoietic tissue factor pathway inhibitor mitigates bleeding in mice with hemophilia. *Proc Natl Acad Sci U S A*. 2012; **109**: 3927-31. 10.1073/pnas.1119858109.

62 Maroney SA, Cooley BC, Ferrel JP, Bonesho CE, Mast AE. Murine hematopoietic cell tissue factor pathway inhibitor limits thrombus growth. *Arterioscler Thromb Vasc Biol.* 2011; **31**: 821-6. 10.1161/ATVBAHA.110.220293.

63 Ellery PE, Maroney SA, Cooley BC, Luyendyk JP, Zogg M, Weiler H, Mast AE. A balance between TFPI and thrombin-mediated platelet activation is required for murine embryonic development. *Blood.* 2015; **125**: 4078-84. 10.1182/blood-2015-03-633958.

Figure legends:

Fig. 1. Similar kinetics of neutrophil recruitment in *Bambi*-deficient mice after laser induced thrombosis model in vivo. (A-B) Representative composite fluorescence images of platelets (green) and neutrophils (red) (left panels) or neutrophils only (right panels) with bright field images after the laser injury in cremaster arterioles of Bambi^{+/+} (A) and Bambi^{/-} mice (B). Platelets and neutrophils were visualized by injecting rat anti-GPIbB-DyLight 488 and rat anti-Ly6G-PE antibodies, respectively. A yellow color is seen when platelets and neutrophils are detected in the same thrombus region. Scale bar represents 10 µm. (C) Graph represents median integrated fluorescence intensity (IFI) from platelets (arbitrary units: AU) as a function of time after the injury. (23-25 thrombi in 3 mice for each genotype). The area under the curve of fluorescence intensity over 180 seconds was analyzed using an unpaired Mann Whitney test; * p<0.05 (D) Number of emboli (>25% maximal thrombus size) counted during 3 min after laser injury. Results are shown as mean ± SEM. Statistical analysis was performed using unpaired student t test. ** p<0.01. (E) Graph represents median neutrophil-IFI (AU) as a function of time after the laser injury. The area under the curve of fluorescence intensity over 180 seconds was analyzed using an unpaired Mann Whitney test; ns: p>0.05. See also Movie S1.

Fig. 2. PECAM-1, ICAM-1 and ICAM-2 are normally expressed in *Bambi¹⁻* MLEC. *Bambi^{+/+}* MLEC and *Bambi¹⁻* MLEC were isolated and cultured on gelatin-coated plates. (A) Representative flow cytometry analysis of *Bambi^{+/+}* MLEC and *Bambi^{-/-}* MLEC for endothelial markers PECAM-1, ICAM-1 and ICAM-2. (B) Results are given as mean fluorescence intensities (MFI) \pm SEM (n \geq 10 from 3 separate isolations; passages 2-8). Statistical analysis was performed using unpaired student t test: non-significant (ns), p>0.05.

Fig. 3. Lack of fibrin(ogen) accumulation in *Bambi^{/-}* thrombi after laser-induced thrombosis model. (A-B) Representative composite fluorescence images of platelets (green) and fibrin (red) (left panels) or fibrin only (right panels) with bright field images after the laser injury in cremaster arterioles of Bambi^{+/+} and Bambi^{+/-} mice. Platelets and fibrin were visualized by injecting rat anti-GPlbβ-DyLight 488 antibody and fibrinogen-A647, respectively. Scale bar represents 10 µm. (C) Graph represents median integrated fluorescence intensity (IFI) from platelets (arbitrary units: AU) as a function of time after the injury (45 thrombi in 7 Bambi^{+/+} mice; 26 thrombi in 4 Bambi^{/-} mice). The area under the curve of fluorescence intensity over 180 seconds was analyzed using an unpaired Mann Whitney test; * p<0.05. (D) Number of emboli (>25% maximal thrombus size) counted during 3 min after laser injury. Results are shown as mean ± SEM. Statistical analysis was performed using unpaired t test, * p<0.05. (E) Graph represents median fibrin(ogen)-IFI (AU) as a function of time after the laser injury. The area under the curve of fluorescence intensity over 180 seconds was analyzed using an unpaired Mann Whitney test, * p<0.05. See also Movie S2 for better visualization of the differences in thrombus stability between Bambi^{+/+} and Bambi^{/-} mice.

Fig. 4. Hirudin-injected *Bambi*^{+/+} **mice exhibit thrombus instability similar to** *Bambi*^{+/-} **mice after laser-induced thrombosis model. (A-B)** Representative composite fluorescence images of platelets (green) with bright field images after the laser injury in cremaster arterioles of *Bambi*^{+/+} and *Bambi*^{-/-} mice. Platelets were visualized by injecting rat anti-GPIbβ-DyLight 488 antibody. Scale bar represents 10 µm. (C-D) For each mouse, 4-5 thrombi were performed prior and after hirudin injection via the jugular vein. *Bambi*^{+/+} mice (n=6) (-hirudin n=29 thrombi; +hirudin n=20 thrombi); *Bambi*^{-/-} mice (n=7) (-hirudin n=37 thrombi; +hirudin n=30 thrombi). **(C)** Graph represents median integrated fluorescence intensity (IFI) from platelets (arbitrary units: AU) as a function of time after the injury. The area under the curve of fluorescence intensity over 180 seconds was analyzed using an unpaired Mann Whitney test; * p<0.05. (D) Number of emboli (>25% maximal thrombus size)

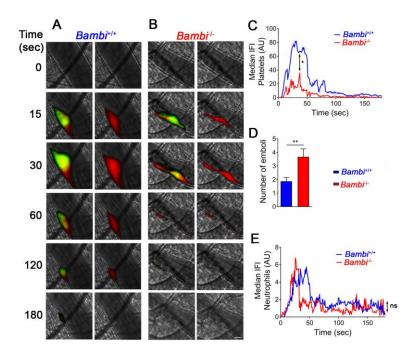
counted during 3 min after laser injury. Results are shown as mean \pm SEM. Statistical analysis was performed using unpaired t test; * p<0.05; ** p<0.01. See Movie S3 for better visualization of the differences in thrombus stability between control group (wild-type mice, no hirudin) and *Bambi^{/-}* or hirudin-injected mice.

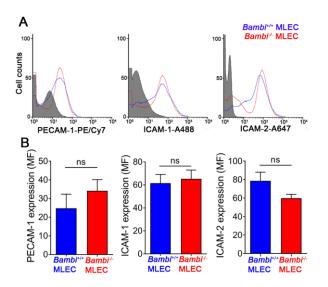
Fig. 5. Endothelial BAMBI is responsible for the defect in thrombus stability *in vivo.* **(A)** Representative composite fluorescence images of platelets (green) and fibrin (red) with bright field images after the laser injury in cremaster arterioles of *Bambi*^{flox/flox} and *Bambi*^{flox/flox} *Tie2-Cre+* mice. Platelets and fibrin were visualized by injecting rat anti-GPlbβ-DyLight 488 antibody and fibrinogen-A647, respectively. Scale bar represents 10 µm. **(B)** Graph represents median integrated fluorescence intensity (IFI) from platelets (arbitrary units: AU) as a function of time after the injury (26 thrombi in 4 *Bambi*^{flox/flox} mice; 28 thrombi in 5 *Bambi*^{flox/flox} *Tie2-Cre+* mice). The area under the curve of fluorescence intensity over 180 seconds was analyzed using an unpaired Mann Whitney test; ns: p>0.05. **(C)** Number of emboli (>25% maximal thrombus size) counted during 3 min after laser injury. Results are shown as mean ± SEM. Statistical analysis was performed using unpaired t test; * p<0.05. **(D)** Graph represents median fibrin(ogen)-IFI (AU) as a function of time after the laser injury. The area under the curve of fluorescends was analyzed using an unpaired median fibrin set in the second set of the set of fluorescence using unpaired t test; * p<0.05. **(D)** Graph represents median fibrin(ogen)-IFI (AU) as a function of time after the laser injury. The area under the curve of fluorescence intensity over 180 seconds was analyzed using an unpaired time set of the second set of the second set of the set of fluorescence intensity over 180 seconds was analyzed using an unpaired median fibrin(ogen)-IFI (AU) as a function of time after the laser injury. The area under the curve of fluorescence intensity over 180 seconds was analyzed using an unpaired to the curve of fluorescence intensity over 180 seconds was analyzed using an unpaired Mann Whitney test; * p<0.05. See also Movie S4.

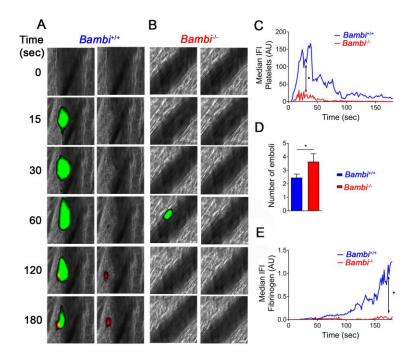
Fig. 6. Increased thrombomodulin and TFPI expression levels in *Bambi^{/-}* mice (A-B) Representative western blot of TFPI (A) and thrombomodulin (B) expression in *Bambi*^{+/+} and Bambi^{/-} lung homogenates. Protein levels were quantified using Image Lab 5.2.1 software (Biorad), normalised against GAPDH controls and expressed as relative intensities (TFPI or TM/GAPDH). Values are given as mean \pm SEM (n \geq 7 mice per genotype from at least 2 western blots). Statistical analysis was performed using unpaired student *t*-test; *p<0.05; **p<0.01. Molecular weights from protein standards are indicated in kDa on each westernblot. (C) Bambi^{+/+} and Bambi^{/-} MLEC were incubated with 100nM human protein C in the presence of Ca²⁺ and activated by 2nM thrombin. The reactions were stopped at the indicated times by addition of an excess of hirudin (100nM). APC generation was quantified by determining the rate of chromogenic substrate S-2366 (0.5mM) cleavage at 405nm and using an APC standard curve generated in parallel for each experiment (cf. Fig. S5D). APC generation was normalised to the number of cells and maximal APC activity for each assay. When indicated (+ α -TM), *Bambi*^{+/+} and *Bambi*^{/-} MLEC were incubated for 30 min with a goat anti-mouse thrombomodulin antibody (50nM) before addition of protein C and thrombin to the wells and APC activity was determined after 60 min. Values are given as mean ± SEM (n=2 separate isolations). Statistical analysis was performed using Two-way ANOVA followed by Bonferroni post-tests; * p<0.05 **p<0.01

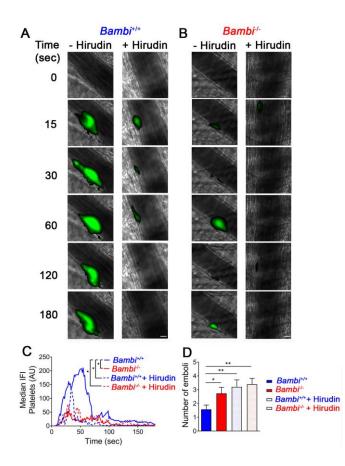
Fig. 7. Inhibiting thrombomodulin and TFPI *in vivo* in *Bambi^{/-}* mice restores thrombus stability and fibrin generation in the laser-induced thrombosis model. (A) Representative composite fluorescence images of platelets (green) and fibrin (red) with bright field images after the laser injury in cremaster arterioles of *Bambi^{+/+}* and *Bambi^{-/-}* mice injected with control goat IgGs, goat anti-mouse thrombomodulin antibody (α -TM), goat anti-mouse TFPI (α -TFPI) or a combination of both α -TM and α -TFPI. Platelets and fibrin were visualized by injecting rat anti-GPIb β -DyLight 488 antibody and fibrinogen-A647, respectively. Scale bar represents 10 µm. (B) Graph represents median integrated fluorescence intensity (IFI) from platelets (arbitrary units: AU) as a function of time after the injury. Thrombi from *Bambi^{+/+}* and *Bambi^{-/-}* mice injected with control goat IgG are overlaid with thrombi from mice injected with α -TM (Bi), α -TFPI (Bii) or a combination of both α -TM and α -TFPI antibodies (Biii) (43 thrombi in 7 *Bambi^{+/+}* mice (+ Goat IgG); 45 thrombi in 6

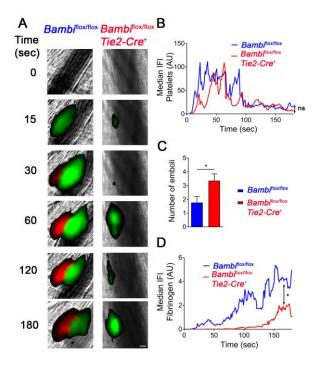
Bambi^{/-} mice (+ Goat IgG); 25 thrombi in 3 *Bambi*^{+/+} mice (+ α-TM); 27 thrombi in 3 *Bambi*^{/-} mice (+ α-TFPI); 28 thrombi in 3 *Bambi*^{+/-} mice (+ α-TFPI); 20 thrombi in 2 *Bambi*^{+/+} mice (+ α-TFPI + α-TM); 20 thrombi in 2 *Bambi*^{+/-} mice (+ α-TFPI + α-TM); 20 thrombi in 2 *Bambi*^{+/-} mice (+ α-TFPI + α-TM). The area under the curve of fluorescence intensity over 180 seconds was analyzed using an unpaired Mann Whitney test; ns: p>0.05. **(C)** Number of emboli (>25% maximal thrombus size) counted during 3 min after laser injury. Results are shown as mean ± SEM. Statistical analysis was performed using one-way ANOVA with Dunnett's multiple comparisons test; vs *Bambi*^{+/+} in Ci. or vs *Bambi*^{-/-} in Cii. * p<0.05. **(D)** Graph represents fibrin(ogen)-IFI (AU) as a function of time after the laser injury. Di. *Bambi*^{+/+} mice injected with Goat IgGs, α-TM, α-TFPI, α-TFPI and α-TM antibodies. Dii. *Bambi*^{+/-} mice injected with Goat IgGs, α-TM, α-TFPI, α-TFPI and α-TM antibodies. The area under the curve of fluorescence intensity over 180 seconds was analyzed using an unpaired Mann Whitney test; ** p<0.01; * p<0.05; ns: p>0.05. See also Movies S5 and S6 for better visualization of the differences in thrombus stability between *Bambi*^{+/+} and *Bambi*^{-/-} mice.

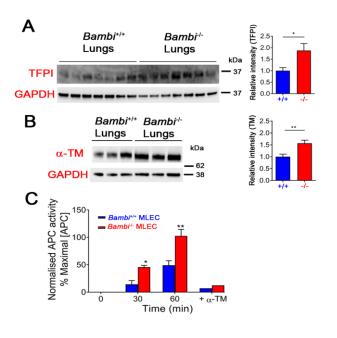


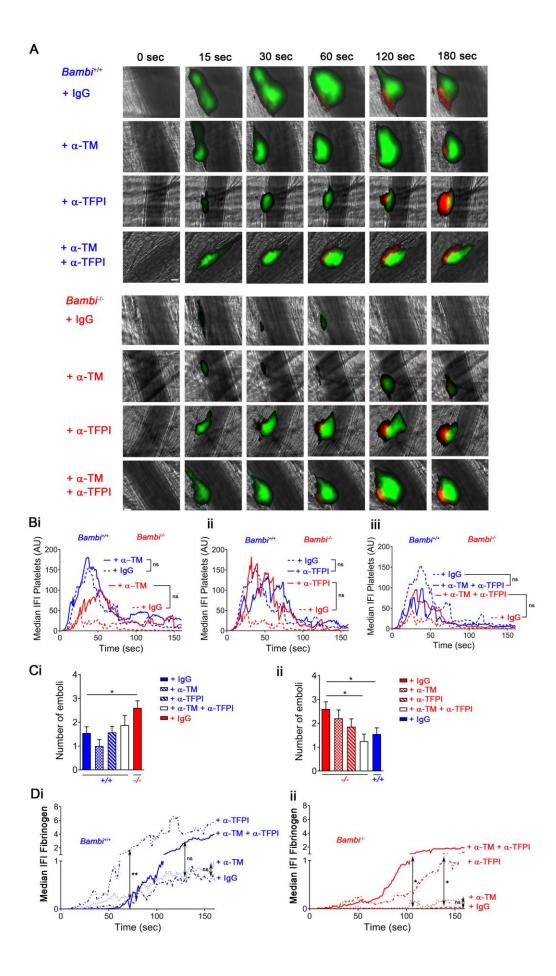












This article is protected by copyright. All rights reserved.